Assessment of vapor–liquid equilibrium models for ionic liquid based working pairs in absorption cycles

Wang, Meng; Becker, Tim; Infante Ferreira, Carlos

DOI
10.1016/j.ijrefrig.2017.09.021

Publication date
2018

Document Version
Final published version

Published in
International Journal of Refrigeration

INTERNATIONAL JOURNAL OF REFRIGERATION 87 (2018) 10–25

Available online at www.sciencedirect.com

ScienceDirect

journal homepage: www.elsevier.com/locate/ijrefrig

Assessment of vapor–liquid equilibrium models for ionic liquid based working pairs in absorption cycles

Meng Wang *, *Tim M. Becker*, *Carlos A. Infante Ferreira*

Process and Energy Department, Delft University of Technology, Leeghwaterstraat 39, 2628 CB Delft, The Netherlands

ARTICLE INFO

Article history:
Received 26 April 2017
Received in revised form 23 August 2017
Accepted 25 September 2017
Available online 14 October 2017

Keywords:
Absorption cycle
Ionic liquid
Mixing enthalpy
VLE
EOS
Activity coefficient model

ABSTRACT

This paper assesses the performance of vapor–liquid equilibrium (VLE) models in ionic liquid based absorption cycles with natural refrigerants. Frequently used equation-of-state (EOS) based models, activity coefficient based models, and generic Clausius–Clapeyron relations are evaluated. Working pairs considered are H_2O/[emim][DMP] and NH_3/[bmim][BF_4]. Firstly, experimental VLE data of those working pairs are correlated by using the models. Mixing enthalpies are then estimated using the models and corresponding correlated parameters. Performances of the different models in reproducing VLE data and estimating mixing enthalpies are compared with each other. Subsequently, total enthalpies and thermodynamic performances of absorption refrigeration cycles are predicted based on the different models. The assessment reveals that the RK-EOS and the NRTL model perform best in reproducing VLE data. In addition, the RK-EOS and the UNIFAC model show the best performance in estimating mixing enthalpies. Hence, the RK-EOS is recommended in correlating VLE data and estimating mixing enthalpies in absorption cycles.

Évaluation de modèles d'équilibre liquide-vapeur pour les paires fonctionnant avec du liquide ionique dans les cycles à absorption

Mots clés : Cycle d'absorption ; Liquide ionique ; Enthalpie de mélange ; Équilibre liquide-vapeur ; Équation d'état ; Modèle de coefficient d'activité

* *Corresponding author.* Process and Energy Department, Delft University of Technology, Leeghwaterstraat 39, 2628 CB Delft, The Netherlands.
E-mail address: M.Wang-2@tudelft.nl (M. Wang).

Abbreviation: C–C, Clausius–Clapeyron equation; EOS, equation of state; G^e, activity coefficient model; G–H, Gibbs–Helmholtz equations; IL, ionic liquid; IS, ideal solution; NRTL, non-random two-liquid model; PR, Peng–Robinson EOS; PRWS, Peng–Robinson EOS with Wong–Sandler mixing rules; PRVdW, Peng–Robinson EOS with van der Waals mixing rules; RK, Redlich–Kwong EOS; TCM, thermodynamically consistent model; UNIFAC, UNIQUAC functional-group activity coefficients method; VLE, vapor–liquid equilibrium; [bmim][BF_4], 1-butyl-3-methylimidazolium tetrafluoroborate; [emim][DMP], 1-ethyl-3-methylimidazolium dimethylphosphate

https://doi.org/10.1016/j.ijrefrig.2017.09.021
0140-7007/

Nomenclature

COP	coefficient of performance [-]
c_p	specific heat capacity [kJ kmol^{-1}K^{-1}]
F	object function [-]
$\bar{f}$	fugacity [MPa]
f	circulation ratio [-]
g	specific Gibbs energy [kJ mol^{-1}]
$h/\Delta h$	specific enthalpy (difference) [kJ mol^{-1}]
$\dot{m}$	mass flow rate [kg s^{-1}]
N	counting number [-]
P	pressure [MPa]
R	molar gas constant [8.314472 J mol^{-1}K^{-1}]
r	correlation coefficient [-]
RMSD	root-mean-square deviation [-]
T	temperature [K/°C]
w	mass concentration [kg kg^{-1}]
x/y	molar concentration in liquid/vapor [mol mol^{-1}]
Z	compressibility factor [-]

Greek symbols

α	interaction parameters in UNIFAC [-]
β	input parameters in RK-EOS [-]
γ	activity coefficient [-]
ϕ	fugacity coefficient [-]
Φ	Poynting correction [-]
ω	acentric factor [-]

Subscript and superscript

0	reference state
1	component of refrigerant
abs	absorption
c	critical point
calc	calculated data
cond	condensation
e	excess properties
evap	evaporation
exp	experimental data
gen	generation
H_2O	H_2O component
i	*i*-th component/point
ig	properties in the ideal gas state
IL	ionic liquid component
L	liquid phase
mix	mixing properties
NH_3	NH_3 component
r	refrigerant stream
real	real properties
res	residual properties
s	strong (of refrigerant) solution stream
sat	saturated state properties
sol	solution
V	vapor phase
w	weak (of refrigerant) solution stream

1. Introduction

Climate change requires humans to keep optimizing the way the energy sector is developing. The ambition of the recent Paris Agreement is accelerating this development (International Energy Agency, 2016). As a clean and renewable way of energy utilization, thermally activated absorption refrigeration and heat pump systems provide opportunities for low-grade heat utilization. Absorption systems show potential in waste heat recovery (Thekdi and Nimbalkar, 2015) and solar thermal cooling and heating (Kim and Infante Ferreira, 2008; International Energy Agency, 2013).

Binary mixtures such as H_2O/LiBr and NH_3/H_2O have been widely used in absorption systems for decades, but many challenges do exist, such as the possibilities of crystallization of the H_2O/LiBr pair (Wang et al., 2011) and the difficulty in separation of the NH_3/H_2O pair (Vasilescu and Infante Ferreira, 2014). Thus, the investigation of alternative absorbents is still a relevant topic (Sun et al., 2012; Vasilescu and Infante Ferreira, 2014). Ionic liquids (ILs), a family of molten salts at room temperature, possess negligible vapor pressure, high thermal and chemical stability, a wide temperature range of liquid state and good solubility of gases (Vega et al., 2010). These key properties meet the requirements (Nowaczyk and Steimle, 1992) for working fluids and make them particularly attractive as potential absorbents in absorption systems (Ayou et al., 2014), especially with natural refrigerants such as H_2O (Dong et al., 2012) and NH_3 (Yokozeki and Shiflett, 2007a, 2007b).

Vapor–liquid equilibrium (VLE) properties and their models play significant roles in the performance analysis of absorption cycles with these novel working pairs. Firstly, they are used to correlate and predict the relationship between pressure, temperature and composition of working pairs. This is usually applied as the first step in performance evaluations, such as working pair screening and determination of state point conditions. The correlated VLE models can also be used to estimate the mixing enthalpy of the working pair, which is an essential part of the total enthalpy. The term mixing enthalpy quantifies the heat effect during mixing of liquid components, which is defined as the difference between the total enthalpy of the solution and its ideal counterpart (Van Ness, 1964),

$$\Delta h_{mix} = h^{sol} - \sum_i x_i h_i \quad (1)$$

VLE models applied in absorption cycles in recent studies are reviewed as follows. For the H_2O based pair H_2O/[emim][DMP], Yokozeki and Shiflett (2010) measured and analyzed VLE data of plentiful H_2O/ILs working pairs using the generic Redlich–Kwong (RK) equation of state (EOS) model and applied this model in the absorption cycle analysis. Wang et al. (2010), Wu et al. (2011), Ren et al. (2011) and Nie et al. (2012) measured and correlated vapor pressure data for other H_2O/ILs pairs with the NRTL model. The correlated NRTL model of Ren et al. (2011) has also been used to study the performance of absorption chillers (Zhang and Hu, 2011) and absorption heat

Table 1 – VLE models applied for the estimation of mixing enthalpy in H_2O/IL and NH_3/IL-based absorption cycles.

Working fluids*	Application	Model for the excess enthalpy	Researcher	Source of VLE data
H_2O/[emim][DMP]	Absorption refrigeration cycle	NRTL	Zhang and Hu (2011)	Ren et al. (2011)
	Absorption heat transformer cycle	NRTL	Zhang and Hu (2012)	
H_2O/[dmim][DMP]	Absorption refrigeration cycle	NRTL	Dong et al. (2012)	Dong et al. (2012)
H_2O/[emim][Tf_2N]	Absorption refrigeration cycle	NRTL	Kim et al. (2012b)	Kato and Gmehling (2005)
H_2O/[emim][BF_4]	Absorption refrigeration cycle	NRTL		Seiler et al. (2004)
H_2O/[bmim][BF_4] H_2O/[emim][BF_4] H_2O/[emim][$C_2H_5SO_4$] H_2O/[mmim][$(CH_3)_2PO_4$] H_2O/[bmim][I] H_2O/[choline][Gly] H_2O/[choline][CH_3SO_3] H_2O/[choline][Lac] H_2O/[bmim][$(C_4H_9)_2PO_4$] H_2O/[eeim][$(C_2H_5)_2PO_4$] H_2O/[emim][$(C_2H_5)_2PO_4$] H_2O/[emim][$(CH_3)_2PO_4$]	Absorption refrigeration cycle	RK-EOS	Yokozeki and Shiflett (2010)	Yokozeki and Shiflett (2010)
NH_3/[bmim][PF_6] NH_3/[hmim][Cl] NH_3/[emim][Tf_2N] NH_3/[bmim][BF_4]	Absorption refrigeration cycle	RK-EOS	Yokozeki and Shiflett (2007a)	Yokozeki and Shiflett (2007a)
NH_3/[emim][Ac] NH_3/[emim][SCN] NH_3/[emim][$EtOSO_3$] NH_3/[DMEA][Ac]	Absorption refrigeration cycle	RK-EOS	Yokozeki and Shiflett (2007b)	Yokozeki and Shiflett (2007b)
NH_3/[bmim]Zn_2Cl_5	Absorption refrigeration cycle	UNIFAC	Chen et al. (2014)	Chen et al. (2013)
NH_3/[choline][NTf_2] NH_3/[emim][Ac] NH_3/[emim][$EtSO_4$] NH_3/[emim][SCN] NH_3/[HOemim][BF_4] NH_3/[hmim][Cl]	Absorption refrigeration cycle	COSMO-RS	Ruiz et al. (2014)	N/A

* Nomenclature of ILs is according to the original works.

transformers (Zhang and Hu, 2012). Dong et al. (2012) used their own correlated NRTL model for the estimation of mixing enthalpy in an investigation of an absorption refrigeration cycle with the H_2O/[dmim][DMP] pair. Kim et al. (2012b) explored a miniature absorption refrigeration cycle with working pairs consisting of different refrigerants and imidazolium-based ILs, including H_2O/[emim][Tf_2N] and H_2O/[emim][BF_4] working pairs. The correlated NRTL model was used for VLE determination and mixing enthalpy estimation. However, in their following work (Kim et al., 2012a, 2013), the NRTL model was replaced by the generic RK-EOS model, which is the same model Yokozeki and Shiflett (2007a, 2007b, 2010) previously used. Since 2013, the group of Zheng started using the UNIFAC model. They correlated the previous VLE experimental data of H_2O/ILs pairs (Dong et al., 2013; Zheng et al., 2013) with the UNIFAC model to quantify the interaction parameters. In terms of NH_3, Yokozeki and Shiflett (2007a, 2007b) applied the generic RK-EOS model in their work to correlate experimental VLE data and to estimate the mixing enthalpy for ammonia based pairs, after they pointed out that an accurate estimation of the mixing enthalpy with the NRTL model is difficult (Shiflett and Yokozeki, 2006). Additionally, Chen et al. (2014) implemented a self-correlated UNIFAC model (Chen et al., 2013) to estimate the mixing enthalpy for an NH_3/IL-based absorption cycle. Ruiz et al. (2014) modeled NH_3/ILs absorption cycles making use of the COSMO-based Aspen thermodynamic properties estimation. The COSMO-RS model was used to estimate properties of non-database components. Previous studies which used VLE models to estimate the mixing enthalpies for H_2O/IL and NH_3/IL working pairs is listed in Table 1.

It is obvious that the NRTL, RK-EOS and UNIFAC models have been frequently used to correlate experimental VLE data and to estimate the mixing enthalpies of working pairs for absorption cycles. All these mentioned models can be regarded as thermodynamically consistent models (TCMs). They were also classified into a family of Gibbs–Helmholtz (G–H) equations by Mathias and O'Connell (2012) and Mathias (2016), which bridges the phase equilibrium with the enthalpy change.

$$\frac{h}{R} = \left.\frac{d(g/RT)}{d(1/T)}\right|_p \qquad (2)$$

Depending on the particular equation applied in the description of the equilibrium, the forms can be different. The current methods of mixing enthalpy estimation can be sorted into the following groups: EOS methods (Eq. (3)), activity coefficient, G^e, (Eq. (4)) methods and C–C method (Eq. (5)), the general forms of them are as follows, respectively,

$$\frac{h_i^{res}}{R} = -\frac{\partial \ln \bar{f}_i}{\partial (1/T)}\bigg|_{p,x} \tag{3}$$

$$\frac{h^e}{R} = \frac{d(g^e/RT)}{d(1/T)}\bigg|_{p,x} \tag{4}$$

$$\frac{\Delta h}{R} = \frac{\partial \ln P}{\partial (1/T)} \tag{5}$$

They are mathematically derived from the fundamental thermodynamic relations, see details in Mathias and O'Connell (2012) and Mathias (2016). The right sides of these TCMs are related to the equilibrium properties, and the left side gives enthalpy changes. Functionally similar to the Gibbs–Duhem equation, these TCMs can be used for:

1. Property estimation, when having the VLE data to predict energy data or vice versa.
2. Consistency analysis, when having both VLE and excess enthalpy data.

In this work, various thermodynamic models are used to correlate the same experimental VLE data of two refrigerant/IL working pairs, H_2O/[emim][DMP] and NH_3/[bmim][BF_4]. The performance of these models is examined. The models considered here include EOS models, activity coefficient models and the general Clausius–Clapeyron relations. Following the thermodynamic consistency, performances of different models in estimating mixing enthalpies and total enthalpies are also evaluated. The estimated values from different models are compared with each other. For H_2O/[emim][DMP], experimental values are also included. Finally, these VLE models are applied to calculate the performance of an absorption cycle, to test how the precision of the model influences the prediction of the cycle performance. This systematic assessment of VLE models is intended to provide essential information for the selection of models in IL-based absorption cycles.

2. Approaches and VLE models

The procedure of the assessment in this study can be summarized as follows:

1. Reliable VLE data are applied to correlate the corresponding VLE models. The correlation performance is evaluated by comparing the deviations. The preferred model gives a low value for the root-mean-square deviation (*RMSD*) between experimental data and predicted values. A high value of the squared correlation coefficient (r^2) would confirm the quality of the correlations.
2. VLE data from independent sources of the same working pairs are adopted to verify the reproducibility of the correlations, and to allow for an uncertainty analysis of the experimental VLE data.
3. Using corresponding models, mixing enthalpies are estimated based on the correlated interaction parameters obtained previously in Step 1.

As mentioned in the introduction in Section 1, there are 3 different alternative methods for the estimation of Δh_{mix} from VLE data by VLE models. In contrast to the method based on the C–C relations, the EOS and G^e methods rely on interaction parameters correlated from VLE data. Thus, the method of VLE calculation is first introduced.

2.1. VLE calculation

The equilibrium criterion is the starting point of VLE calculations. Its general form can be expressed by using the fugacities $\bar{f}$ of both liquid and vapor phases (Sandler, 2006),

$$\bar{f}_i^L(T, P, x_i) = \bar{f}_i^V(T, P, y_i) \tag{6}$$

When using EOS methods, the equilibrium criterion can be stated as in Eq. (7). This procedure is also referred to as $\phi - \phi$ method,

$$x_i \bar{\phi}_i^L(T, P, x_i) = y_i \bar{\phi}_i^V(T, P, y_i) \tag{7}$$

The fugacity coefficients ϕ for both phases can be obtained from the EOS.

Another description of VLE uses an activity coefficient for the liquid phase and an EOS for the vapor phase. This method is usually referred to as the $\gamma - \phi$ method.

$$x_i \gamma_i(T, P, x_i) P_i^{sat}(T) \Phi_i = y_i P \bar{\phi}_i^V(T, P, y_i) \tag{8}$$

In the case of refrigerant/IL systems, due to the non-volatility of IL, its fraction in the vapor phase can be neglected, i.e. $y_1 = 1$. The equilibrium pressure of the binary system is relatively low, especially when compared with the critical pressure of refrigerants. Therefore, the Poynting correction Φ can be considered to be unity. The fugacity coefficient of the refrigerant component in the vapor phase, $\bar{\phi}_1^V$, can also be approximated to be 1 due to the ideal behavior of the vapor at low pressure. Following these assumptions, Wang et al. (2010) and Ren et al. (2011) implemented the equilibrium criterion as,

$$\gamma_1 = \frac{P}{x_1 P_1^{sat}} \tag{9}$$

For the VLE models discussed in this work, the same set of experimental data is used to regress the unknown interaction parameters. The nonlinear-least-square method is implemented to correlate the data. The objective function F in Eq. (10) is chosen as the difference between experimental liquid phase fugacity values and calculated ones using the models.

$$F = \sum_{i=1}^{N} \left(\bar{f}_{1,i}^{\exp L} - \bar{f}_{1,i}^{calcL} \right)^2 \tag{10}$$

2.2. Mixing enthalpy estimation

2.2.1. Mixing enthalpy estimated from EOS models

The first method for the estimation of Δh_{mix} is to use a specific EOS model. After obtaining the interaction parameters in the mixing rules, the general form of residual enthalpy, h^{res}, can be expressed as Eq. (11),

$$h^{res} = RT^2 \int_{P_0}^{P} \left(\frac{\partial Z}{\partial T}\right)_P \frac{dP}{P} \tag{11}$$

where Z is the compressibility factor, the form of which depends on the particular EOS. The residual enthalpy, h^{res}, is defined as the difference between the ideal gas enthalpy and the real one.

$$h^{res} = h^{ig} - h^{real} \tag{12}$$

With the residual enthalpies of the mixture and both the pure components at liquid state, the mixing enthalpy can be calculated via

$$\Delta h_{mix} = \sum_{i=1}^{N} x_i h_i^{res} - h_{sol}^{res} \tag{13}$$

In this study, the PR-EOS with van der Waals mixing rules (PRVdW) (Peng and Robinson, 1976), PR-EOS with Wong–Sandler mixing rules (PRWS) (Wong and Sandler, 1992) and a modified RK-EOS (Yokozeki and Shiflett, 2007b) were included in the evaluation. The details of these models can be found in the Appendix.

2.2.2. *Mixing enthalpy estimated from G^e models*

The second method is to use G^e models. With a G^e model and the corresponding regressed binary interaction VLE parameters, the excess Gibbs energy can be obtained by

$$\frac{g^e}{RT} = \sum_{i=1}^{N} x_i \ln \gamma_i \tag{14}$$

The relationship between excess enthalpy and excess Gibbs energy is defined by Eq. (4). Together with Eq. (14), the excess enthalpy can be obtained.

G^e models only work for solutions, thus, the excess enthalpy calculated by Eq. (4) is actually the mixing heat (Chen et al., 2014; Dong et al., 2012). G^e models considered here are the NRTL (Dong et al., 2012) and the UNIFAC (Dong et al., 2013) models. The details of these models can also be found in the Appendix.

2.2.3. *Mixing enthalpy estimated from C–C equation*

The third method to estimate the Δh_{cond} is to use the C–C equation. In an lnP-(-1/T) diagram, the slope of the curve reflects the heat effect during phase-change:

$$\frac{d \ln P}{d(1/T)} = -\frac{\Delta h}{R} \tag{15}$$

Table 2 – Inputs for the PR-EOS (PRVdW and PRWS models in this study)*.

Compound	T_c [K]	P_c [MPa]	ω [-]
H_2O	647.1	22.06	0.3443
[emim][DMP]	836.85	2.50	0.6383
NH_3	406.15	11.42	0.25601
[bmim][BF_4]	643.18	2.04	0.8877

* PRVdW and PRWS models are discussed in Peng and Robinson (1976) and Wong and Sandler (1992), respectively. Critical points and acentric factors are predicted using the group-function method proposed by Valderrama and Robles (2007).

For the vapor pressure curve of a pure fluid, Δh is the latent heat Δh_{cond} (Kiss and Infante Ferreira, 2016). When it concerns the vapor pressure of a mixture with fixed concentration, Δh is the absorption heat Δh_{abs} (Meyer et al., 2015). Note that the mixing enthalpy is the heat effect during the mixing of two liquid components, which can be obtained by removing the latent heat from the absorption heat,

$$\Delta h_{mix} = \Delta h_{abs} - \Delta h_{cond} \tag{16}$$

2.3. *Fluids information of working pairs in VLE models*

Except for the NRTL model, the application of VLE models in VLE calculation and the estimation of the Δh_{mix} require input information. For instance, the critical information and acentric factors are required for the EOS based models. In the case of UNIFAC models, group volumes, area parameters and some interaction parameters of/between split functional groups are needed. H_2O/[emim][DMP] and NH_3/[bmim][BF_4] working pairs were selected because the required input information of these pairs is available in literature. Tables 2–5 list the used information and the corresponding references for each model discussed in this study.

3. Results and discussion

3.1. *Performance in correlating and reproducing VLE data*

3.1.1. *H_2O/[emim][DMP] pair*

The H_2O/[emim][DMP] pair is one of the few working pairs for which experimental mixing enthalpy data have been published. For this working pair, the VLE data reported by Ren et al. (2011) are used for the correlation. The authors collected the experimental data at 5 different concentrations, see Fig. 1.

Table 3 – Inputs for the RK-EOS*.

Compound	T_c [K]	P_c [MPa]	β_0 [-]	β_1 [K]	β_2 [MPa]	β_3 [-]
H_2O	647.1	22.06	1.00236	0.54254	−0.08667	0.00525
[emim][DMP]	852.21	1.81	1	To be correlated	0	0
NH_3	406.15	11.42	1.00027	0.45689	−0.05772	0
[bmim][BF_4]	894.9	3.02	1	To be correlated	0	0

* The RK-EOS studied in this work and its input parameters are discussed in Yokozeki and Shiflett (2007a, 2010).

Table 4 – Group volumes and area parameters used in the UNIFAC model*.

Group	Volumes [-]	Surface area [-]
H_2O	0.92	1.4
NH_3	1.4397	2.0918
CH_2	0.6744	0.54
CH_3	0.9011	0.848
[mim][DMP]	6.2609	4.996
$[mim][BF_4]$	6.5669	4.005

* Group division of working fluids is discussed in Lei et al. (2009) and Dong et al. (2013).

Table 5 – Group interaction parameters used in the UNIFAC model*.

Group 1	Group 2	a_{12} [-]	a_{21} [-]
H_2O	CH_2/CH_3	300	1318
H_2O	[mim][DMP]	To be correlated $gi_1(1)$	To be correlated $gi_3(1)$
CH_2/CH_3	[mim][DMP]	To be correlated $gi_2(1)$	To be correlated $gi_4(1)$
NH_3	CH_2/CH_3	To be correlated $gi_1(2)$	To be correlated $gi_3(2)$
NH_3	$[mim][BF_4]$	To be correlated $gi_2(2)$	To be correlated $gi_4(2)$
CH_2/CH_3	$[mim][BF_4]$	1108.51	588.74

* Group division of working fluids is discussed in Lei et al. (2009) and Dong et al. (2013).

Different VLE models are correlated based on the VLE data. The correlated interaction parameters and the qualities of the correlations of different models are listed in Table 6. The qualities are quantified using the root-mean-square deviation (*RMSD*), the maximum relative deviation (*Max.Dev.*) of data points, and by the squared correlation coefficient (r^2) between the measured and correlated pressures (which reflects the degree of linearity of the correlations). The predicted VLE curves of the H_2O/[emim][DMP] pair are also illustrated in Fig. 1(a–e) for the corresponding VLE models.

The studied models seem to be able to reproduce the VLE data of the H_2O/[emim][DMP] working pair. The prefered models, RK-EOS and NRTL models, perform the best because they give low values for the *RMSD* between experimental and predicted values.

The previous correlations were only based on the VLE data reported by Ren et al. (2011). VLE data from the other independent source (Wang et al., 2007) are also applied to check the uncertainty of the previous correlations. Similarly, the root-mean-square deviation (*RMSD*) and the squared correlation coefficient (r^2) are adopted to verify the reproduction qualities, as listed in Table 7.

Even though the reproducibility of the independent data is worse than reproducing the same data used for the correlation, the performances of most models are still acceptable, especially for the RK and NRTL models with lower *RMSD* values.

3.1.2. $NH_3/[bmim][BF_4]$ pair

VLE data of the $NH_3/[bmim][BF_4]$ pair, which were reported by Yokozeki and Shiflett (2007a), for 5 isothermal conditions are

Table 6 – Correlation results and performances of different models by using VLE data of H_2O/[emim][DMP] pair reported by Ren et al. (2011).

Correlated coefficients*		Correlation performance†		
		RMSD	*Max.Dev.*	r^2
PRVdW	−0.796; −0.282	5.53%	11.35%	0.970
PRWS	0.576; 0.591; −15.080; −2.679	3.99%	7.14%	0.986
RK	0.174; −17.584; 0.038; 0.015; 0.608	2.43%	9.21%	0.997
NRTL	0.434; 0.454; 350.924; −2.261; −388.387	2.63%	7.08%	0.996
UNIFAC	−590.684; −686.639; −460.958; 1780.121	4.55%	10.17%	0.983

* Coefficients of PRVdW are k_{12} (=k_{21}) and l_{12} (=l_{21}) respectively (Kiss and Infante Ferreira, 2016); Coefficients of PRWS are k_{12}, α, $\tau_{12}^{(0)}$ and $\tau_{21}^{(0)}$ respectively (Ramdin et al., 2013); Coefficients of RK are β_1, τ_{12} (=τ_{21}), l_{12}, l_{21} and m_{12} (=m_{21}) respectively (Yokozeki and Shiflett, 2007b); Coefficients of NRTL are α, $\tau_{12}^{(0)}$, $\tau_{12}^{(1)}$, $\tau_{21}^{(0)}$ and $\tau_{21}^{(1)}$ respectively (Dong et al., 2012); Coefficients of UNIFAC are the group interaction parameters ($gi_1(1)$-$gi_4(1)$) mentioned in Table 5.

† $RMSD(P) = \sqrt{\frac{\sum_N (P_{fit}/P_{exp} - 1)^2}{N}}$, represents the root-mean-square deviation. *Max.Dev.* is the maximum relative deviation of data points. r^2 is the squared correlation coefficient between the measured and correlated pressures.

Table 7 – VLE data reproducibility of the H_2O/[emim][DMP] pair (Wang et al., 2007) by using the correlated models based on VLE data reported by Ren et al. (2011).

	RMSD	r^2
PRVdW	14.08%	0.976
PRWS	12.49%	0.982
RK	9.16%	0.965
NRTL	9.56%	0.965
UNIFAC	10.60%	0.966

plotted in Fig. 2. The correlated interaction parameters and the correlations performances of the different models for this pair are listed in Table 8. Generally, the errors are larger than those for the H_2O/[emim][DMP] pair. However, the RK-EOS and NRTL models still show the best performance, while the performance of the UNIFAC model is the worst. The predicted isotherms of the $NH_3/[bmim][BF_4]$ pair are also illustrated in Fig. 2(a–e) for the corresponding VLE models.

VLE data reported by Li et al. (2010) are applied here as an independent source to verify the reproducibility of the previous correlations based only on data of Yokozeki and Shiflett (2007a). As listed in Table 9, the reproducibility of this pair is not as good as one of the H_2O/[emim][DMP] pair. Nevertheless, the reproduction qualities, especially of the ones based on NRTL model, are still acceptable.

3.2. *Performance in the estimation of mixing enthalpies*

3.2.1. H_2O/[emim][DMP] pair

For the H_2O/[emim][DMP] working pair, the estimated mixing enthalpies using the different models at $T = 298.15$ K and

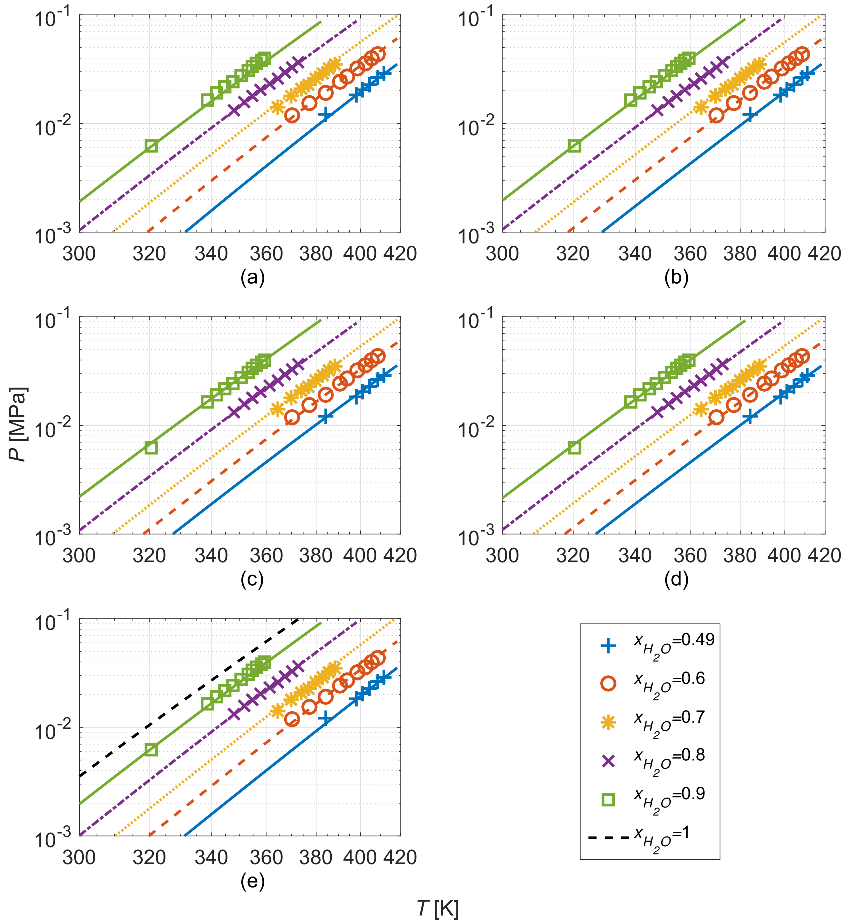

Fig. 1 – Experimental VLE data of the H_2O/[emim][DMP] pair as reported by Ren et al. (2011) and the correlated VLE curves at constant H_2O concentration via different models: (a) PRVdW, (b) PRWS, (c) RK, (d) NRTL, and (e) UNIFAC.

P = 0.1 MPa (for G^e and C–C methods, only $T = 298.15$ K is required) are shown in Fig. 3 along with the experimentally measured ones (Ren et al., 2011; Zhang et al., 2014).

All estimated values show obvious deviations from the measured ones. The RK-EOS, UNIFAC and NRTL models estimate the experimental data the best. The mixing enthalpies estimated with the PRVdW model are positive while the other models show negative values. For conditions $x_{H_2O} < 0.5$, the results estimated with the C–C relation require extrapolation of the experimental data. This results in an outlier for $x_{H_2O} = 0.18$.

3.2.2. *NH_3/[bmim][BF_4] pair*

The VLE data of the NH_3/[bmim][BF_4] pair were measured at 5 isothermal conditions. When using the C–C method, an additional step is required to obtain the data at different concentrations. Fig. 4 shows how the data have been processed. The experimental VLE data including the vapor pressure data of pure NH_3 are first fitted to a polynomial. Vapor pressure data at constant concentrations (0.1–0.9 of NH_3 molar concentration) were then interpolated, see Fig. 4(a). The interpolated data are again plotted in an lnP-(-1/T) diagram, see Fig. 4(b), for the experimental temperature range. The slopes of these curves are used to estimate the absorption and mixing heat with Eq. (15) and (16). This data processing inevitably introduces additional errors.

Estimated Δh_{mix} values at $T = 298.15$ K and P = 1.1 MPa (for G^e and C–C methods, only $T = 298.15$ K is required) are shown in Fig. 5. Note that for the given conditions, the pure NH_3 is in a liquid state and hence the latent heat is not taken into account here. The values for the PRVdW and PRWS models are significantly larger than the others, and are not presented. The two G^e models, i.e. NRTL and UNIFAC, produce contradicting trends. The RK-EOS model and the C–C relation show intermediate values. Δh_{mix} values estimated from C–C and RK-EOS change from positive to negative. This behavior indicates that the mixing of the two liquid components is exothermic at low ammonia concentration while endothermic at high ammonia concentration. The differences in the estimated Δh_{mix} values at the same condition are significant.

A thorough search of the relevant literature still yielded no work on the mixing enthalpy data of solution NH_3/[bmim][BF_4], thus the judgment of which model is more suitable for this pair is not possible currently. Nevertheless, compared with Δh_{mix} values of the H_2O/[emim][DMP] pair, absolute values of Δh_{mix} for the NH_3/[bmim][BF_4] pair are generally much lower. This indicates smaller heat effects during the mixing of liquid NH_3 with [bmim][BF_4].

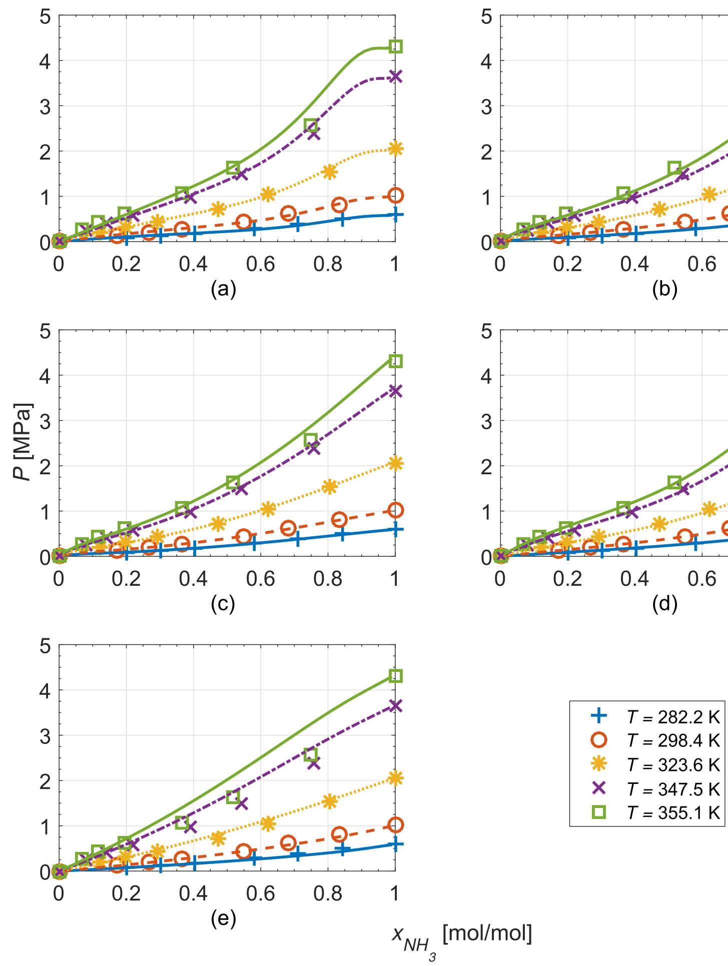

Fig. 2 – Experimental VLE data of the NH_3/[bmim][BF_4] pair as reported by Yokozeki and Shiflett (2007a) and the correlated VLE isotherms via different models: (a) PRVdW, (b) PRWS, (c) RK, (d) NRTL, and (e) UNIFAC.

Table 10 summarizes the key information of the models considered in this study and their performances in respect to the estimation of Δh_{mix}.

3.2.3. *Outlooks of molecular simulation*

Besides the discussed models here, molecular simulations can be used to predict the mixing enthalpy of IL working pairs. In molecular simulations, thermodynamic properties are calculated based on a potential which describes the molecular interactions. These potentials are often correlated to experimental VLE data similar to the models discussed in this work, but can also be used to extrapolate mixture properties from pure component data. Previously, Maginn and colleagues explored these methods to calculate the mixing enthalpy of H_2O/[emim][$EtSO_4$] (Kelkar et al., 2008) and NH_3/[emim][Tf_2N] (Shi and Maginn, 2009). While the initial results for H_2O/[emim][$EtSO_4$] did not agree well with experimental measurements, these authors slightly adjusted the potential to better reproduce experimental results. Moreover, these authors suggested more sophisticated potentials to further improve the accuracy of molecular simulations. Hence, we see molecular simulations as an alternative approach.

3.3. *Total enthalpy calculation*

3.3.1. *H_2O/[emim][DMP] solution*

Depending on the availability of the heat capacities of the IL-based solutions, there are two alternative methods to calculate the total enthalpy. If the heat capacity of the solution, c_p^{sol}, is known, its total enthalpy at a specified temperature and concentration can be calculated from

$$h^{sol}(T, x_1) = h^{sol}(298.15, x_1) + \int_{298.15}^{T} c_p^{sol}(x_1)\,dT \tag{17}$$

where $h^{sol}(298.15, x_1)$ is the solution enthalpy at 298.15 K and a concentration of x_1. Based on an arbitrarily chosen reference state, here at 273.15 K, this enthalpy can be calculated via,

$$h^{sol}(298.15, x_1) = \Delta h_{mix}(298.15, x_1) + x_1 \int_{273.15}^{298.15} c_p^{IL}\,dT + (1 - x_1) \int_{273.15}^{298.15} c_p^{H_2O}\,dT \tag{18}$$

Table 8 – Correlation results and performances of different models by using VLE data of NH_3/[bmim][BF_4] pair reported by Yokozeki and Shiflett (2007a).

Correlated coefficients*		Correlation performance†		
		RMSD	Max.Dev.	r^2
PRVdW	−0.036; 0.517	10.32%	25.52%	0.992
PRWS	0.633; −7.206; 0.233; 0.363	5.06%	11.79%	0.998
RK-EOS	0.771; -3.104; −0.017; −0.074; 0.028	4.68%	11.72%	0.997
NRTL	−0.011; −52.253; 9597.721; 36.085; −6024.139	2.82%	7.87%	0.997
UNIFAC	296.011; 210.119; −316.806; −316.844	14.64%	16.45%	0.987

* Coefficients of PRVdW are k_{12} (=k_{21}) and l_{12} (=l_{21}) respectively (Kiss and Infante Ferreira, 2016); Coefficients of PRWS are k_{12}, α, $\tau_{12}^{(0)}$ and $\tau_{21}^{(0)}$ respectively (Ramdin et al., 2013); Coefficients of RK are β_1, τ_{12} (=τ_{21}), l_{12}, l_{21} and m_{12} (=l_{21}) respectively (Yokozeki and Shiflett, 2007b); Coefficients of NRTL are α, $\tau_{12}^{(0)}$, $\tau_{12}^{(1)}$, $\tau_{21}^{(0)}$ and $\tau_{21}^{(1)}$ respectively (Dong et al., 2012); Coefficients of UNIFAC are the group interaction parameters ($gi_1(2)$-$gi_4(2)$) mentioned in Table 5.

† $RMSD(P) = \sqrt{\frac{\sum_N (P_{fit}/P_{exp} - 1)^2}{N}}$, represents the root-mean-square deviation. *Max.Dev.* is the maximum relative deviation of data points. r^2 is the squared correlation coefficient between the measured and correlated pressures.

For the H_2O/[emim][DMP] working pair, total enthalpies at 328.15 K are calculated using $\Delta h_{mix}(298.15, x_1)$ from different models. The results are presented in Fig. 6. Heat capacities of pure IL and solutions reported by Zhang and Hu (2011) were also used in the calculation. The properties of H_2O were taken from the NIST database (Lemmon et al., 2013).

The ideal solution, IS, in which the effects of mixing enthalpy are neglected is also shown in Fig. 6. Only mixing enthalpies calculated by the PR-EOS and the C–C relation, see Fig. 3, have positive deviations. Compared with the total enthalpy calculated using the experimental mixing enthalpies, the UNIFAC and RK models agree the best, while the comparable deviations are in opposite directions. The largest deviation occurs at a concentration around $x_1 = 0.7$–0.8.

The previous method of the total enthalpy calculation only requires mixing enthalpy data at one temperature condition, while it also needs heat capacities of the solution. For most IL-based pairs, especially in the absorbent screening phase, the heat capacities of the solutions are not available. Therefore, the previously presented total enthalpy calculation method is not

Table 9 – VLE data reproducibility of the NH_3/[bmim][BF_4] pair (Li et al., 2010) by using the correlated models based on VLE data reported by Yokozeki and Shiflett (2007a).

	RMSD	r^2
PRVdW	29.4%	0.963
PRWS	36.8%	0.972
RK	37.9%	0.974
NRTL	27.3%	0.971
UNIFAC	23.6%	0.952

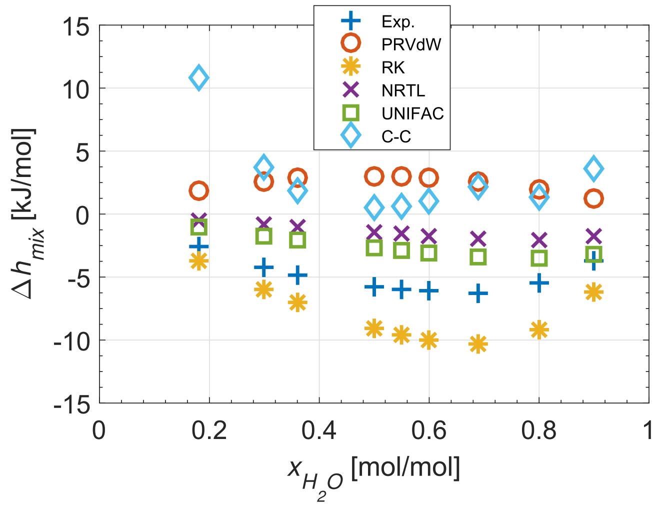

Fig. 3 – Comparison of the experimental and the estimated Δh_{mix} values for the H_2O/[emim][DMP] pair at T = 298.15 K and P = 0.1 MPa.

applicable. As an alternative, the following method which directly uses the mixing enthalpy and the enthalpy of the IS can be applied (Chen et al., 2014; Kim et al., 2012a).

$$h^{sol}(T, x) = \Delta h_{mix}(T, x) + x_1 \int_{T_0}^{T} c_p^{IL} dT + (1 - x_1) \int_{T_0}^{T} c_p^{H_2O} dT \quad (19)$$

In Fig. 7, the total enthalpies calculated using both methods are displayed along the horizontal axis and the vertical axis, respectively. All points are displayed along the $x = y$ line. The behavior indicates that the two methods can be used alternatively to calculate the total enthalpies for the H_2O/[emim][DMP] solution. Furthermore, the result implies that the excess heat capacity of the solution, i.e. the difference between the heat capacity of the real solution and its ideal counterpart, has a very limited influence, because Eq. (19) neglects the excess heat capacity.

3.3.2. NH_3/[bmim][BF_4] solution

Fig. 8 shows the results of total enthalpies of the NH_3/[bmim][BF_4] solution when the mixing enthalpies obtained by the different sources are used. Eq. (19) has been used because there are no published heat capacity data for this solution. In comparison to the H_2O/[emim][DMP] solution, a smaller deviation can be observed between the ideal solution and the enthalpy values obtained with the different models. This is because the Δh_{mix} of the NH_3/[bmim][BF_4] pair is smaller.

3.4. *Influence on the absorption cycle performance*

Two factors resulting from VLE models can lead to different predictions of the performance of an absorption cycle. One is the influence of the model on the determination of operating conditions. If the solubility is incorrectly predicted, the cycle performance will be inaccurate. The second aspect is the mixing enthalpy estimation, which is of significance for the estimation of the total enthalpy. The circulation ratio, f, one of the

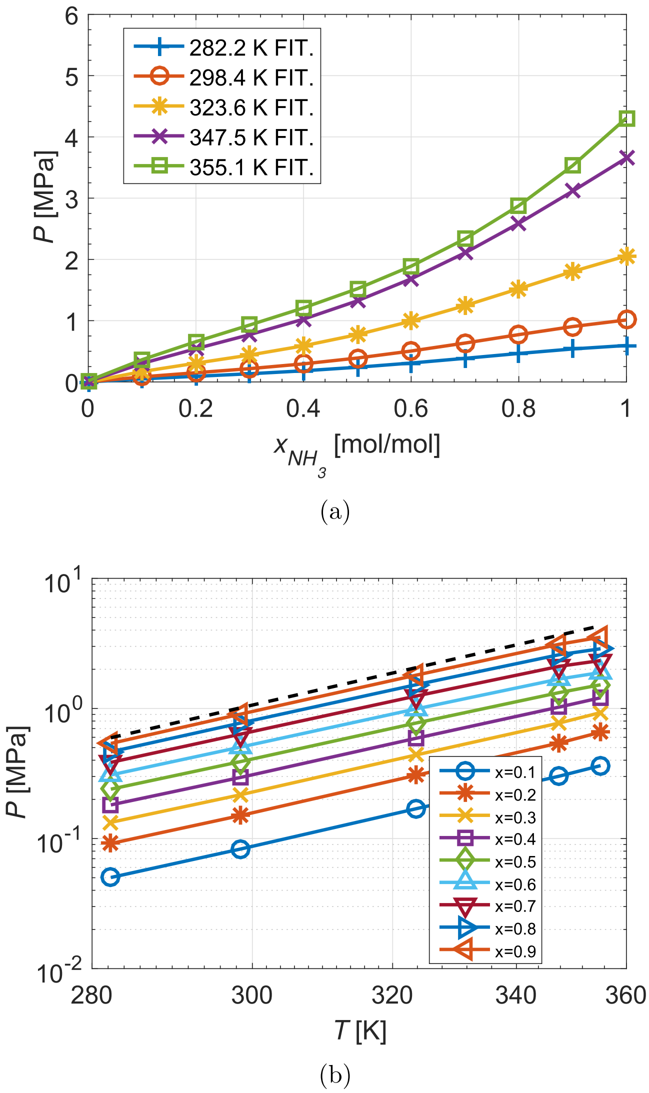

Fig. 4 – VLE data processing before using Clausius–Clapeyron relations. (a) Interpolation at constant concentrations. (b) The interpolated data shown in an *ln*P-(-1/T) diagram (dash line represents the saturated pressure of pure NH_3).

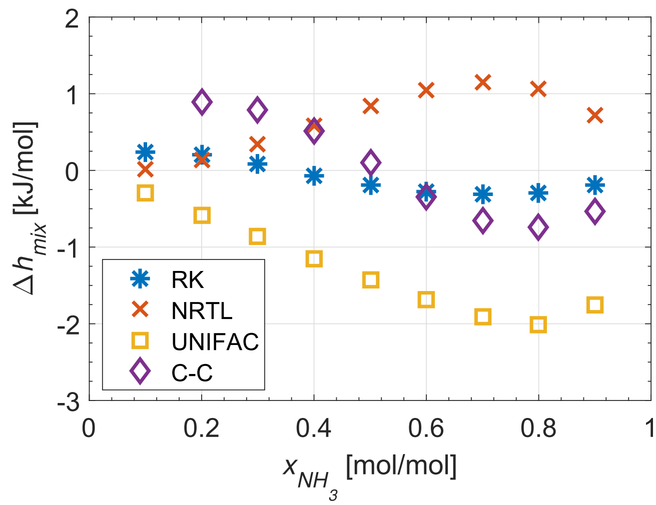

Fig. 5 – Comparison between the Δh_{mix} estimated with the different estimation methods for the NH_3/[bmim][BF_4] working pair at $T = 298.15$ K and $P = 1.1$ MPa.

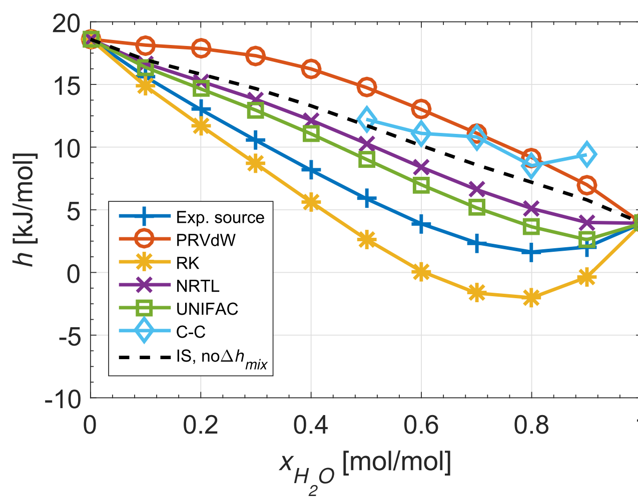

Fig. 6 – Comparison of the total enthalpies of the H_2O/[emim][DMP] solution at 328.15 K as estimated by the different VLE models. The lines distinguish sources of the mixing enthalpies for the estimation of total enthalpies.

performance criteria, reflects solely the effect of the VLE correlation, while the coefficient of performance (*COP*) reflects the effects of both factors. In the following, the comparison of these two performance criteria is presented when the different models are used.

The cycle configuration and its thermodynamical description were introduced in previous work by the authors (Wang and Infante Ferreira, 2017). In this study, both working pairs are applied in an absorption refrigeration system operating

Table 10 – Summary of Δh_{mix} estimation using the different VLE models for the H_2O/[emim][DMP] pair.

Type	Model	Δh_{mix} estimation method	Remarks
EOS	PRVdW	$\ln \bar{f}_i \rightarrow h_i^{res} \rightarrow \Delta h_{mix}$	Critical information and acentric factors needed, sign of heat effect does not agree with experiments
	PRWS		Critical information and acentric factors needed, large deviations from experiments
	RK		Critical information needed, one the two best performing models
G^e	NRTL	$\ln\gamma_i \rightarrow g^e \rightarrow h^e(\Delta h_{mix})$	No input needed, close to UNIFAC model
	UNIFAC		Group information needed, one of the best performing methods
	C–C	$\ln P_i \rightarrow \Delta h_{abs} \rightarrow \Delta h_{mix}$	No input needed, second largest deviation

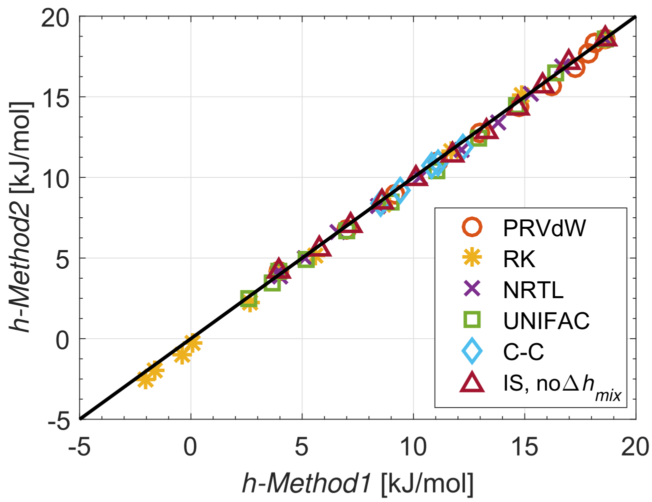

Fig. 7 – Comparison of the two methods for the calculation of the total enthalpies of H_2O/[emim][DMP] solution at 328.15 K. h-Method1 is based on Eq. (17) and (18), while h-Method2 is based on Eq. (19). The symbols distinguish sources of the mixing enthalpies for the estimation of total enthalpies.

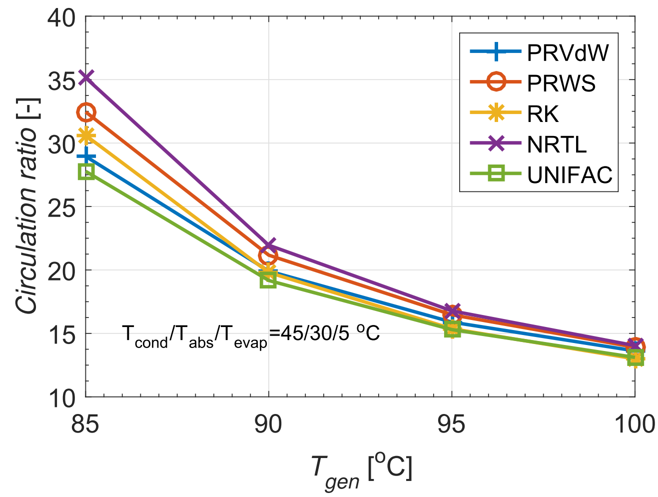

Fig. 9 – Calculated circulation ratio of the H_2O/[emim][DMP] working pair in an absorption refrigeration cycle by different VLE models. The lines distinguish sources of the VLE prediction.

under the conditions $T_{cond}/T_{abs}/T_{evap} = 45/30/5$ °C. The heat source temperature T_{gen} varies from 85 to 100 °C.

The circulation ratio, f, which is defined as the mass flow ratio between the pump stream and the refrigerant stream can be obtained using mass and species balances,

$$f = \frac{\dot{m}_s}{\dot{m}_r} = \frac{1 - w_w}{w_s - w_w} \tag{20}$$

Fig. 9 presents the results of f for the absorption cycle with H_2O/[emim][DMP] working pair. These results are obtained when applying the different VLE models. f is solely quantified by the solubilities obtained from the VLE data. The results of f do not show large differences, because they are based on the same set of VLE experimental data.

Using the enthalpy calculation methods discussed in Section 3.3, the COP, defined as a ratio between the cooling effect obtained in the evaporator and the heat input to the generator, can be calculated. Fig. 10 shows the estimated COP for varying levels of heat source temperature. Since there is no sensible difference in f, the difference in the predicted COPs is mainly due to the difference in mixing enthalpies. Results based on ideal solutions and experimental mixing enthalpy data are also plotted as references.

Generally, the models that estimate higher mixing enthalpies lead to a higher predicted COP. This relationship implies that a less exothermic effect during mixing is preferable for

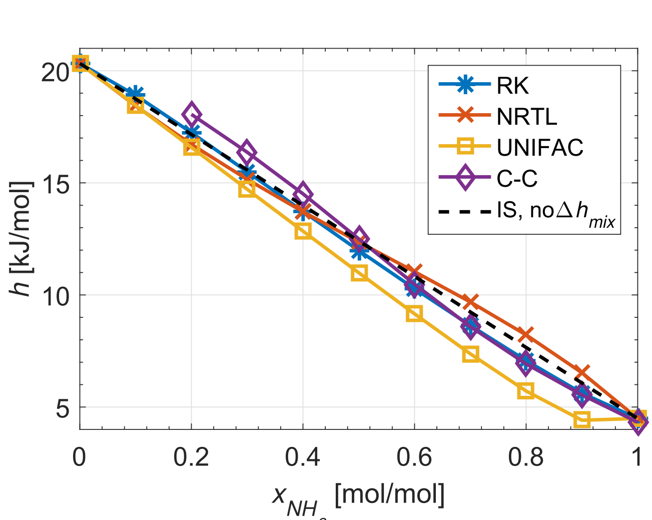

Fig. 8 – Comparison of the total enthalpies at 328.15 K of the NH_3/[bmim][BF_4] solution estimated by different VLE models. The lines distinguish sources of the mixing enthalpies for the estimation of total enthalpies.

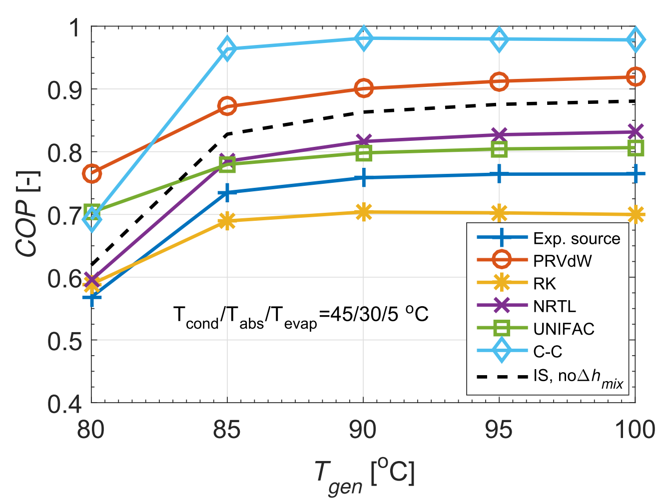

Fig. 10 – Calculated coefficient of performance of the H_2O/[emim][DMP] working pair in an absorption refrigeration cycle when the different VLE models are applied. The lines distinguish sources of the VLE prediction and the mixing enthalpy estimation.

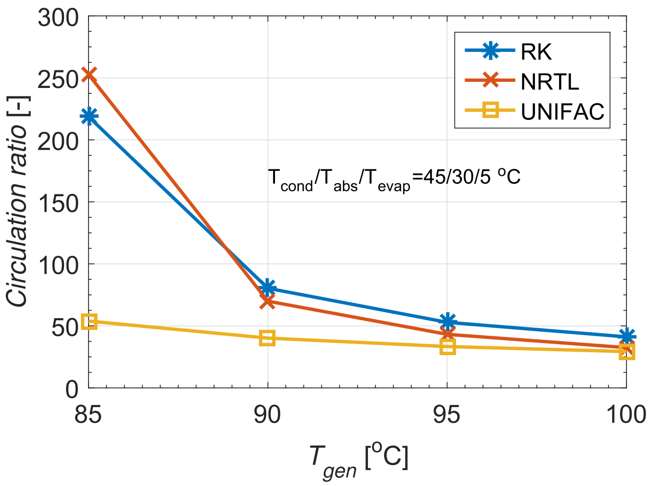

Fig. 11 – Calculated circulation ratio of the NH_3/[bmim][BF_4] working pair in an absorption refrigeration cycle by different VLE models. The lines distinguish sources of the VLE prediction.

the absorption cycle. The highest *COP* is attained when using the C–C model. Thereby, it is shown that a steep change of the mixing enthalpy can lead to an overestimated performance.

Similar to the mixing enthalpy estimation, RK-EOS and UNIFAC models also present the closest predictions for *COP* values compared with the one using experimental data. However, the *COP* values predicted using these two models are distributed on both sides of the experimental predicted *COP*.

The *f* and *COP* values of the absorption refrigeration cycle for the NH_3/[bmim][BF_4] working pair are also calculated, see Figs. 11 and 12. Large differences for *f* can be observed at a lower generation temperature (85 °C): The UNIFAC model gives a lower value of *f*, which leads to a higher estimation of *COP*. This is mainly due to the relatively poor performance in reproducing

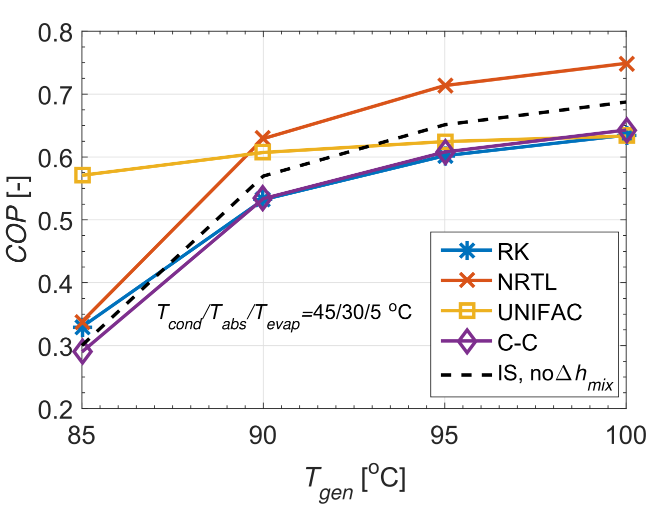

Fig. 12 – Calculated coefficient of performance of the NH_3/[bmim][BF_4] working pair in an absorption refrigeration cycle when the different VLE models are applied. The lines distinguish sources of the VLE prediction and the mixing enthalpy estimation.

the VLE data, as listed in Table 8. For high generation temperatures, RK-EOS, UNIFAC and C–C models show similar values for the *COP*, while all results are lower than the ones for the ideal solution. The NRTL model overestimates the *COP*. The relation between the cycle performance and the estimated values of Δh_{mix} agrees with the previous observations for the cycle using H_2O/[emim][DMP] as working pair. Additionally, the *COP* values of the cycle with NH_3/[bmim][BF_4] working pair are lower than the ones for the H_2O/[emim][DMP] pair.

4. Conclusion

The performance of different VLE models applied to ionic liquid based absorption refrigeration cycles has been evaluated for the two investigated working pairs (H_2O/[emim][DMP] and NH_3/[bmim][BF_4]). Specifically:

- For the sake of analyzing absorption cycles when no experimental data is available for the mixing enthalpy, the Redlich–Kwong equation of state performs best in both correlating VLE data and estimating mixing enthalpies. Besides, the NRTL model is also suitable for the correlation of VLE data and the UNIFAC model can be applied for estimating mixing enthalpies.
- The mixing of liquid NH_3 with [bmim][BF_4] is less exothermic since the absolute values of Δh_{mix} for this pair are smaller than those of the H_2O/[emim][DMP] pair.
- The results of total enthalpies for the H_2O/[emim][DMP] solution are more sensitive to the VLE models compared to the NH_3/[bmim][BF_4] solution.
- Excess effects in the heat capacity of solutions are not dominant. This has been shown by comparing two alternative methods for the calculation of total enthalpies for the H_2O/[emim][DMP] solution.
- Performance parameters (*f* and *COP*) of the absorption refrigeration cycle vary when using different VLE models. The variation of *COP* is larger for the cycle with the H_2O/[emim][DMP] pair. For the same working pair, a model estimating a smaller Δh_{mix} (more exothermic effect) would underestimate the *COP*.

Acknowledgment

The authors would like to acknowledge the financial support from the China Scholarship Council, (Scholarship 201406320184).

Appendix

Appendix A:EOS and activity coefficient models

Peng–Robinson (PR) EOS
The basic expression of Peng–Robinson EOS is (Peng and Robinson, 1976),

$$P = \frac{RT}{V-b} - \frac{a(T)}{V(V+b)+b(V-b)} \tag{A.1}$$

where V is the molar volume, R is the gas constant. The parameters a and b here are defined as,

$$a(T) = 0.457235\frac{R^2T_c^2}{P_c}\alpha \tag{A.2}$$

$$b = 0.077796\frac{RT_c}{P_c} \tag{A.3}$$

where the subscript c represents the critical conditions of the substance. With ω, the acentric factor and $\alpha(T)$, in classical PR-EOS, are defined as,

$$\alpha^2 = 1 + (0.37646 + 1.54226\omega - 0.26992\omega^2)\left(1 - \frac{T^{0.5}}{T_c}\right) \tag{A.4}$$

As for the mixtures in low pressure cases, conventional quadratic mixing rule (VdW mixing rule) with two interaction parameters is used to describe the behavior as,

$$a_m = \sum_{i,j=1}^{N}\sqrt{a_ia_j}(1 - k_{ij})x_ix_j \tag{A.5}$$

where

$$k_{ij} = k_{ji}, \quad k_{ii} = 0 \tag{A.6}$$

and

$$b_m = \frac{1}{2}\sum_{i,j=1}^{N}(b_i + b_j)(1 - l_{ij})x_ix_j \tag{A.7}$$

where

$$l_{ij} = l_{ji}, \quad l_{ii} = 0 \tag{A.8}$$

The parameters a_i and b_i for all pure components in the mixing rules can be calculated using the aforementioned way for a and b. Thus, there are only two parameters needed to be correlated, i.e., k_{12} and l_{12} for a binary mixture.

For high pressure applications, PR-EOS is usually combined with the Wong–Sandler (WS) mixing rules (Wong and Sandler, 1992), which are given by,

$$b_m = \frac{\sum_{i,j=1}^{N}x_ix_j\left(b - \frac{a}{RT}\right)_{ij}}{1 - \frac{A_\infty^E(x_i)}{CRT} - \frac{\sum_{i=1}^{N}x_ia_i}{b_iRT}} \tag{A.9}$$

$$a_m = b\left(\sum_{i=1}^{N}\frac{x_ia_i}{b_i} + \frac{A_\infty^E(x_i)}{C}\right) \tag{A.10}$$

$$\left(b - \frac{a}{RT}\right)_{ij} = \frac{1}{2}\left[\left(b_i - \frac{a_i}{RT}\right) + \left(b_j - \frac{a_j}{RT}\right)\right](1 - k_{ij}) \tag{A.11}$$

where k_{ij} is a binary interaction parameter ($k_{ij} = k_{ji}$) and the constant C is −0.62322 for PR-EOS. The excess Helmholtz energy at infinite pressure $A_\infty^e(x_i)$ is calculated through the assumption that $A_\infty^e(x_i) \approx A_0^e(x_i) \approx G_0^e(x_i)$. The excess Gibbs energy, $G_0^e(x_i)$, at low pressure can be obtained from an activity coefficient model, here the conventional NRTL model. For the binary solution, the expression of $G_0^e(x_i)$ is,

$$\frac{G_0^e}{RT} = x_1x_2\left(\frac{\tau_{21}G_{21}}{x_1 + x_2G_{21}} + \frac{\tau_{12}G_{12}}{x_2 + x_1G_{12}}\right) \tag{A.12}$$

where, the expressions of G_{21} and G_{12} are given in Eq. (A.23), and the τ_{12} and τ_{21} can be used directly without the dependence of T. In this case, the parameters of this PRWS model to be correlated are k_{12}, α, τ_{12} and τ_{21}.

Generic Redlich–Kwong (RK) EOS

The generic RK type of cubic EOS can be written in the following form (Yokozeki and Shiflett, 2007b),

$$P = \frac{RT}{V - b} - \frac{a(T)}{V(V + b)} \tag{A.13}$$

where a and b are expressed by the following,

$$a(T) = 0.42748\frac{R^2T_c^2}{P_c}\alpha(T) \tag{A.14}$$

and

$$b = 0.08664\frac{RT_c}{P_c} \tag{A.15}$$

where the temperature-dependent part of the parameter α for pure component is modeled by the following empirical form,

$$\alpha(T) = \sum_{k=0}^{\le 3}\beta_k\left(\frac{T_c}{T} - \frac{T}{T_c}\right)^k \tag{A.16}$$

As Yokozeki and Shiflett (2007b) reported, β_2 of ILs can be determined through the binary VLE data analysis with $\beta_0 = 1$ and $\beta_2 = \beta_3 = 0$. β values for the natural refrigerants H_2O and NH_3 along with the critical conditions are summarized in Table 2. For the mixtures, three binary interaction parameters τ, l and k are introduced in the parameters a and b for an N-component system via,

$$a_m = \sum_{i,j=1}^{N}\sqrt{a_ia_j}f_{ij}(T)(1 - k_{ij})x_ix_j \tag{A.17}$$

where, $f_{ij}(T) = 1 + \frac{\tau_{ij}}{T}$, $\tau_{ij} = \tau_{ji}$ and $\tau_{ii} = 0$. $k_{ij} = \frac{l_{ij}l_{ji}(x_i + x_j)}{l_{ji}x_i + l_{ij}x_j}$ and $k_{ii} = 0$.

$$b = \frac{1}{2}\sum_{i,j=1}^{N}(b_i + b_j)(1 - k_{ij})(1 - m_{ij})x_ix_j \tag{A.18}$$

where $m_{ij} = m_{ji}$ and $m_{ii} = 0$.

For the RK-EOS, the fugacity, $\bar{\phi}_i$, could be derived as follows,

$$\ln\bar{\phi}_i = \ln\frac{RT}{P(V-b)} + b_i'\left(\frac{1}{V-b} - \frac{a}{RTb(V+b)}\right) + \frac{a}{RTb}\left(\frac{a_i'}{a} - \frac{b_i'}{b} + 1\right)\ln\frac{V}{V+b} \tag{A.19}$$

where, the explicit forms of a' $\left(a_i' \equiv \left(\frac{\partial na}{\partial n_i}\right)_{n_{j\neq i}}\right)$ and b' $\left(b_i' \equiv \left(\frac{\partial nb}{\partial n_i}\right)_{n_{j\neq i}}\right)$ are respectively,

$$a_i' = 2\sum_{j=1}^{N}\sqrt{a_i a_j}\, f_{ij} x_j\left[1 - k_{ij} - \frac{l_{ij}l_{ji}(l_{ij}-l_{ji})x_i x_j}{(l_{ji}x_i + l_{ij}x_j)^2}\right] - a \tag{A.20}$$

$$b_i' = \sum_{j=1}^{N}(b_i + b_j)(1-m_{ij})x_j\left[1 - k_{ij} - \frac{l_{ij}l_{ji}(l_{ij}-l_{ji})x_i x_j}{(l_{ji}x_i + l_{ij}x_j)^2}\right] - b \tag{A.21}$$

Thus, the parameters that need to be regressed are β_1 for the ILs along with τ_{12}, l_{12}, l_{21} and m_{12} for the mixtures.

Non-random two-liquid (NRTL) model

The non-random two-liquid model is one of the frequently used activity coefficient models. For a binary mixture with a non-volatile component in this study, the model can be expressed as (Dong et al., 2012),

$$\ln\gamma_i = x_2^2\left[\tau_{21}\left(\frac{G_{21}}{x_1 + x_2 G_{21}}\right)^2 + \frac{G_{12}\tau_{12}}{(x_2 + x_1 G_{12})^2}\right] \tag{A.22}$$

where

$$G_{12} = \exp(-\alpha\tau_{12}), \quad G_{21} = \exp(-\alpha\tau_{21}) \tag{A.23}$$

and τ_{ij} is correlated with temperature-dependent expressions,

$$\tau_{12} = \tau_{12}^{(0)} + \frac{\tau_{12}^{(1)}}{T}, \quad \tau_{21} = \tau_{21}^{(0)} + \frac{\tau_{21}^{(1)}}{T} \tag{A.24}$$

The parameters to be correlated in this model are α, $\tau_{12}^{(0)}$, $\tau_{21}^{(0)}$ and $\tau_{12}^{(1)}$, $\tau_{21}^{(1)}$.

UNIFAC model

Before applying the UNIFAC model to the VLE calculation, the molecule of every component of the binary system needs to be split into functional groups. Parameters used in this model are mainly based on the properties of each functional group. As proposed by Kim et al. (2005), Lei et al. (2009) and Dong et al. (2013), H_2O, NH_3 and ILs in this study are divided into groups which are listed in Table A1.

Using the UNIFAC model, the activity coefficient, γ_i, can be obtained from a combination of two terms via (Dong et al., 2013),

$$\ln\gamma_i = \ln\gamma_i^C + \ln\gamma_i^R \tag{A.25}$$

where γ_i^C and γ_i^R denote the combinatorial and residual term of species i, respectively. The combinatorial terms represent the difference of size and shape of the molecules, which could be expressed as,

Table A1 – Group division of the molecules of the studied working pairs.

Molecule	Group division
Water	1 H_2O
[emim][DMP]	1 CH_2, 1 CH_3, 1 [mim][DMP]
Ammonia	1 NH_3
[bmim][BF_4]	3 CH_2, 1 CH_3, 1 [mim][BF_4]

$$\ln\gamma_i^C = 1 - \phi_i + \ln\phi_i - 5q_i\left(1 - \frac{\phi_i}{\theta_i} + \ln\frac{\phi_i}{\theta_i}\right) \tag{A.26}$$

The parameters are defined as,

$$\phi_i = \frac{r_i}{\sum_j r_j x_j}, \quad \theta_i = \frac{q_i}{\sum_j q_j x_j} \tag{A.27}$$

where r_i and q_i, which denote the volume and surface area of the i-th species, are defined as the sum of the group volume and area parameters R_k and Q_k,

$$r_i = \sum_k v_k^{(i)} R_k \tag{A.28}$$

and

$$q_i = \sum_k v_k^{(i)} Q_k \tag{A.29}$$

of which $v_k^{(k)}$ is the number of group k in species i. The values of R_k and Q_k for each functional group in this study are listed in Table 4.

The residual term, can be described in the following form,

$$\ln\gamma_i^R = \sum_k v_k^{(i)}\left(\ln\Gamma_k - \ln\Gamma_k^{(i)}\right) \tag{A.30}$$

where Γ_k is the group residual activity coefficient, and $\Gamma_k(i)$ is the residual activity coefficient of group k in a reference solution containing only molecules of type i. They both are given as,

$$\ln\Gamma_k = Q_k\left[1 - \ln\left(\sum_m \theta_m\varphi_{mk}\right) - \sum_m\left(\frac{\theta_m\varphi_{km}}{\sum_n \theta_n\varphi_{nm}}\right)\right] \tag{A.31}$$

$$\theta_m = \frac{\sum_i v_m^{(i)} x_i}{\sum_i\sum_k v_k^{(i)} x_i} \tag{A.32}$$

$$\varphi_{mn} = \exp\left(-\frac{a_{mn}}{T}\right), \quad (a_{mn} \neq a_{nm}) \tag{A.33}$$

When the group volume and area parameters are available, some of the group interaction parameters, a_{mn}, are the only parameters unknown. Thus, they are the ones to be correlated from the experimental VLE data. The number of the group interaction parameters, a_{mn}, depends on the division of the specific molecules. For this work, all of the known and unknown interaction parameters are listed in Table 5.

REFERENCES

Ayou, D.S., Currás, M.R., Salavera, D., García, J., Bruno, J.C., Coronas, A., 2014. Performance analysis of absorption heat transformer cycles using ionic liquids based on imidazolium cation as absorbents with 2,2,2-trifluoroethanol as refrigerant. Energy Convers. Manag. 84, 512–523.

Chen, W., Liang, S., Guo, Y., Gui, X., Tang, D., 2013. Investigation on vapor-liquid equilibria for binary systems of metal ion-containing ionic liquid [bmim]Zn2Cl5/NH3 by experiment and modified UNIFAC model. Fluid Phase Equilib. 360, 1–6.

Chen, W., Liang, S., Guo, Y., Tang, D., 2014. Thermodynamic analysis of an absorption system using [bmim]Zn2Cl5/NH3 as the working pair. Energy Convers. Manag. 85, 13–19.

Dong, L., Zheng, D., Nie, N., Li, Y., 2012. Performance prediction of absorption refrigeration cycle based on the measurements of vapor pressure and heat capacity of H2O+[DMIM]DMP system. Appl. Energy 98, 326–332.

Dong, L., Zheng, D., Li, J., Nie, N., Wu, X., 2013. Suitability prediction and affinity regularity assessment of H2O+imidazolium ionic liquid working pairs of absorption cycle by excess property criteria and UNIFAC model. Fluid Phase Equilib. 348, 1–8.

International Energy Agency, 2013. Technology roadmap: solar heating and cooling. Tech. rep., OECD/IEA, Paris.

International Energy Agency, 2016. Energy, climate change & environment: 2016 insights. Tech. rep., OECD/IEA, Paris.

Kato, R., Gmehling, J., 2005. Measurement and correlation of vapor–liquid equilibria of binary systems containing the ionic liquids [EMIM][(CF3SO2)2N], [BMIM][(CF3SO2)2N], [MMIM][(CH3)2PO4] and oxygenated organic compounds respectively water. Fluid Phase Equilib. 231 (1), 38–43.

Kelkar, M.S., Shi, W., Maginn, E.J., 2008. Determining the accuracy of classical force fields for ionic liquids: atomistic. Ind. Eng. Chem. Res. 47 (23), 9115–9126.

Kim, D., Infante Ferreira, C., 2008. Solar refrigeration options – a state-of-the-art review. Int. J. Refrigeration 31 (1), 3–15.

Kim, S., Kim, Y.J., Joshi, Y.K., Fedorov, A.G., Kohl, P.A., 2012a. Absorption heat pump/refrigeration system utilizing ionic liquid and hydrofluorocarbon refrigerants. J. Electron. Packag. 134 (3), 15–30.

Kim, S., Patel, N., Kohl, P.A., 2013. Performance simulation of ionic liquid and hydrofluorocarbon working fluids for an absorption refrigeration system. Ind. Eng. Chem. Res. 52 (19), 6329–6335.

Kim, Y., Choi, W., Jang, J., Yoo, K.-P., Lee, C., 2005. Solubility measurement and prediction of carbon dioxide in ionic liquids. Fluid Phase Equilib. 228–229, 439–445.

Kim, Y.J., Kim, S., Joshi, Y.K., Fedorov, A.G., Kohl, P.A., 2012b. Thermodynamic analysis of an absorption refrigeration system with ionic-liquid/refrigerant mixture as a working fluid. Energy 44 (1), 1005–1016.

Kiss, A.A., Infante Ferreira, C.A., 2016. Heat Pumps in Chemical Process Industry. CRC Press.

Lei, Z., Zhang, J., Li, Q., Chen, B., 2009. UNIFAC Model for Ionic Liquids. Ind. Eng. Chem. Res. 48 (5), 2697–2704.

Lemmon, E.W., Huber, M.L., McLinden, M.O., 2013. NIST reference fluid thermodynamic and transport properties-REFPROP.

Li, G., Zhou, Q., Zhang, X., Lei, W., Zhang, S., Li, J., 2010. Solubilities of ammonia in basic imidazolium ionic liquids. Fluid Phase Equilib. 297 (1), 34–39.

Mathias, P.M., 2016. The Gibbs-Helmholtz equation in chemical process technology. Industrial & Engineering Chemistry Research, acs.iecr.5b03405. http://pubs.acs.org/doi/10.1021/acs.iecr.5b03405.

Mathias, P.M., O'Connell, J.P., 2012. The Gibbs–Helmholtz equation and the thermodynamic consistency of chemical absorption data. Ind. Eng. Chem. Res. 51 (13), 5090–5097. http://pubs.acs.org/doi/abs/10.1021/ie202668k.

Meyer, T., Kühn, R., Ricart, C., Zegenhagen, T., Ziegler, F., 2015. Simulation of an absorption refrigerator working with ionic liquids and natural refrigerants. In: Proceedings of the 24th IIR International Congress of Refrigeration. Yokohama, Japan, pp. 1–10.

Nie, N., Zheng, D., Dong, L., Li, Y., 2012. Thermodynamic properties of the water + 1-(2-Hydroxylethyl)-3-methylimidazolium chloride system. J. Chem. Eng. Data 57 (12), 3598–3603.

Nowaczyk, U., Steimle, F., 1992. Thermophysical properties of new working fluid systems for absorption processes. Int. J. Refrigeration 15 (1), 10–15.

Peng, D.-Y., Robinson, D.B., 1976. A new two-constant equation of state. Ind. Eng. Chem. Fund. 15 (1), 59–64. http://pubs.acs.org/doi/abs/10.1021/i160057a011.

Ramdin, M., Olasagasti, T.Z., Vlugt, T.J.H., De Loos, T.W., 2013. High pressure solubility of CO_2 in non-fluorinated phosphonium-based ionic liquids. J. Supercrit. Fluids 82, 41–49.

Ren, J., Zhao, Z., Zhang, X., 2011. Vapor pressures, excess enthalpies, and specific heat capacities of the binary working pairs containing the ionic liquid 1-ethyl-3-methylimidazolium dimethylphosphate. J. Chem. Thermodyn. 43 (4), 576–583.

Ruiz, E., Ferro, V.R., De Riva, J., Moreno, D., Palomar, J., 2014. Evaluation of ionic liquids as absorbents for ammonia absorption refrigeration cycles using COSMO-based process simulations. Appl. Energy 123, 281–291.

Sandler, S., 2006. Chemical, biochemical, and engineering thermodynamics. No. v. 1 In: Chemical, Biochemical, and Engineering Thermodynamics. John Wiley & Sons.

Seiler, M., Jork, C., Kavarnou, A., Arlt, W., Hirsch, R., 2004. Separation of azeotropic mixtures using hyperbranched polymers or ionic liquids. AIChE J. 50 (10), 2439–2454.

Shi, W., Maginn, E.J., 2009. Molecular simulation of ammonia absorption in the ionic liquid 1-ethyl-3-methylimidazolium bis(trifluoromethylsulfonyl)imide ([emim][Tf 2 N]). AIChE J. 55 (9), 2414–2421.

Shiflett, M.B., Yokozeki, A., 2006. Solubility and diffusivity of hydrofluorocarbons in room-temperature ionic liquids. AIChE J. 52 (3), 1205–1219.

Sun, G., Zheng, D., Huang, W., Dong, L., 2012. The measurement of ammonia solubility in the ionic liquid 1, 3-dimethylimidazolium dimethylphosphate ([Dmim] DMP). J. Beijing Univ. Chem. Technol. 39 (4), 17–21.

Thekdi, A., Nimbalkar, S.U., 2015. Industrial waste heat recovery-potential applications, available technologies and crosscutting R&D opportunities. Tech. rep., Oak Ridge National Lab.(ORNL), Oak Ridge, TN.

Valderrama, J.O., Robles, P.A., 2007. Critical properties, normal boiling temperatures, and acentric factors of fifty ionic liquids. Ind. Eng. Chem. Res. 46 (4), 1338–1344.

Van Ness, H., 1964. Property change of mixing. In: Classical Thermodynamics of Non-Electrolyte Solutions. Elsevier, pp. 69–86.

Vasilescu, C., Infante Ferreira, C., 2014. Solar driven double-effect absorption cycles for sub-zero temperatures. Int. J. Refrigeration 39, 86–94.

Vega, L.F., Vilaseca, O., Llovell, F., Andreu, J.S., 2010. Modeling ionic liquids and the solubility of gases in them: recent advances and perspectives. Fluid Phase Equilib. 294 (1–2), 15–30.

Wang, J., Wang, D., Li, Z., Zhang, F., 2010. Vapor pressure measurement and correlation or prediction for water, 1-propanol, 2-propanol, and their binary mixtures with [MMIM][DMP] ionic liquid. J. Chem. Eng. Data 55 (11), 4872–4877.

Wang, J.-F., Li, C.-X., Wang, Z.-H., Li, Z.-J., Jiang, Y.-B., 2007. Vapor pressure measurement for water, methanol, ethanol, and their binary mixtures in the presence of an ionic liquid 1-ethyl-3-methylimidazolium dimethylphosphate. Fluid Phase Equilib. 255 (2), 186–192.

Wang, K., Abdelaziz, O., Kisari, P., Vineyard, E.A., 2011. State-of-the-art review on crystallization control technologies for water/LiBr absorption heat pumps. Int. J. Refrigeration 34 (6), 1325–1337.

Wang, M., Infante Ferreira, C.A., 2017. Absorption heat pump cycles with NH_3 ionic liquid working pairs. Appl. Energy 204 (July), 819–830. http://dx.doi.org/10.1016/j.apenergy.2017.07.074.

Wong, D.S.H., Sandler, S.I., 1992. A theoretically correct mixing rule for cubic equations of state. AIChE J. 38 (5), 671–680. http://doi.wiley.com/10.1002/aic.690380505.

Wu, X., Li, J., Fan, L., Zheng, D., Dong, L., 2011. Vapor pressure measurement of water+1, 3-dimethylimidazolium tetrafluoroborate system. Chin. J. Chem. Eng. 19 (3), 473–477.

Yokozeki, A., Shiflett, M.B., 2007a. Ammonia solubilities in room-temperature ionic liquids. Ind. Eng. Chem. Res. 46 (5), 1605–1610.

Yokozeki, A., Shiflett, M.B., 2007b. Vapor–liquid equilibria of ammonia + ionic liquid mixtures. Appl. Energy 84 (12), 1258–1273.

Yokozeki, A., Shiflett, M.B., 2010. Water solubility in ionic liquids and application to absorption cycles. Ind. Eng. Chem. Res. 49 (19), 9496–9503.

Zhang, X., Hu, D., 2011. Performance simulation of the absorption chiller using water and ionic liquid 1-ethyl-3-methylimidazolium dimethylphosphate as the working pair. Appl. Therm. Eng. 31 (16), 3316–3321.

Zhang, X., Hu, D., 2012. Performance analysis of the single-stage absorption heat transformer using a new working pair composed of ionic liquid and water. Appl. Therm. Eng. 37, 129–135.

Zhang, X., Hu, D., Zhao, Z., 2014. Measurement and prediction of excess enthalpies for ternary solutions 1-ethyl-3-methylimidazolium dimethylphosphate + methanol or ethanol + water at 298.15 K and at normal atmospheric pressure. J. Chem. Eng. Data 59 (2), 205–211.

Zheng, D., Dong, L., Wu, X., 2013. New approach for absorbent species selection with excess Gibbs function. Ind. Eng. Chem. Res. 52 (27), 9480–9489.